Metabonomic Investigation of Liver Profiles of Nonpolar Metabolites Obtained from Alcohol-Dosed Rats and Mice Using High Mass Accuracy MS[n] Analysis

Neil Loftus[1], **Alan Barnes**[1], **Simon Ashton**[1], **Filippos Michopoulos**[2,3], **Georgios Theodoridis**[2], **Ian Wilson**[3], **Cheng Ji**[4], and **Neil Kaplowitz**[4]

[1]Shimadzu Corporation, Mass Spectrometry Business Unit, Manchester, UK

[2]Department of Chemistry, Aristotle University of Thessaloniki, 541 24 Greece

[3]AstraZeneca, CPD & DMPK, Mereside, Alderley Park, Macclesfield, Cheshire SK10 4TG UK

[4]Department of Medicine, University of Southern California, Los Angeles, CA, USA

Abstract

Alcoholism is a complex disorder that, in man, appears to be genetically influenced, although the underlying genes and molecular pathways are not completely known. Here the intragastric alcohol feeding model in rodents was used together with high mass accuracy LC/MS[n] analysis to assess the metabonomic changes in nonpolar metabolite profiles for livers from control and alcohol treated rats and mice. Ion signals with a peak area variance of less than 30% (based on repeat analysis of a pooled quality control sample analysed throughout the batch) were submitted to multivariate statistical analysis (using principal components analysis, PCA). PCA revealed robust differences between profiles from control and alcohol-treated animals from both species. The major metabolites seen to differ between control and alcohol-treated animals were identified using high accuracy MS[n] data and verified using external search engines (http://www.lipidmaps.org; http://www.hmdb.ca; http://www.genome.jp/kegg/) and authentic standards. The main metabolite classes to show major changes in the alcoholic liver-derived samples were fatty acyls, fatty acid ethyl esters, glycerolipids and phosphatidylethanol homologues. Significant metabolites that were up-regulated by alcohol treatment in both rat and mouse livers included fatty acyls, metabolites such as octadecatrienoic acid and eicosapentaenoic acid, a number of fatty acid ethyl esters such as ethyl arachidonate, ethyl docosahexaenoic acid, ethyl linoleate and ethyl oleate and phosphatidylethanol (PEth) homologues (predominantly PEth 18:0/18:2 and PEth 16:0/18:2; PEth homologues are currently considered as potential biomarkers for harmful and prolonged alcohol consumption in man). A number of glycerophospholipids resulted in both up-regulation (*m/z* 903.7436 [M+H]$^+$ corresponding to a triglyceride) and down-regulation (*m/z* 667.5296 [M+H]$^+$ corresponding to a diglyceride). Metabolite profiles were broadly similar in both mouse and rat models. However, there were a number of significant differences in the alcohol-treated group particularly in the marked down-regulation of retinol and free cholesterol in the mouse compared to the rat. Unique markers for alcohol treatment included ethyl docosahexaenoic acid.

Metabolites were identified with high confidence using predominantly negative ion MS[n] data for the fatty acyl components to match to www.lipidmaps.org MS and MS/MS databases; interpreting positive ion data needed to take into account possible adduct ions which may confound the

identification of other lipid classes. The observed changes in lipid profiles were consistent with alcohol induced liver injury in humans.

Keywords

Alcohol; ethanol; liver; lipids; metabolite profiling; metabolomics; metabonomics; LC-MS

Introduction

The challenge for global metabolite profiling is to provide novel hypothesis free, but hypothesis generating, insights into the phenotypes of biological systems and the chemical pathways related to disease and toxicity[1⁻3]. A range of analytical tools are now available to bioscientists wishing to generate these metabolic phenotypes (metabotypes[4]) especially those using nuclear magnetic resonance (NMR) spectroscopy and mass spectrometry (MS)-based methods (with the latter most usually hyphenated to a separation system such as gas or liquid chromatography (GC or LC) [5⁻7]).

An important area where metabolic profiling might be expected to inform the understanding of the disease process is alcohol-related liver damage. Alcoholic liver damage has been studied extensively in recent years using the model of intragastric alcohol-fed mice[8⁻11]. This model has a number of advantages in that alcohol can be co-administered with food in a liquid form through a cannula inserted into the stomach and the exposure of the test animal to ethanol can, in this way, be carefully controlled. Recently there have been a number of metabolomic investigations of the effects of alcohol administration to rodents that have used this model based on either ^{1}H NMR spectroscopy[12] or a combination of NMR spectroscopy and direct infusion Fourier transform mass spectrometry (FT-MS)[13] for metabolite profiling. In addition a study based on LC-MS analysis has investigated changes in urine composition on the alcohol-induced changes seen in alcohol-fed male *Ppara*-null mice[14]. Here we describe the results of LC-MS-based metabonomic investigations on the liver metabolomes of rats and mice for the non-polar endogenous metabolites using intragastric alcohol-fed models, with metabolite identification *via* high accuracy MS^n analysis.

Methods

Solvents and Reagents

All solvents used for LC/MS analysis (Chromasolv grade) was purchased from Sigma-Aldrich (Dorset, UK). Adrenic acid, cholesterol, 3-deoxyvitamin D3, ethyl arachidonate, ethyl oleate, formic acid, retinol and retinol palmitate were also purchased from Sigma-Aldrich. For the extraction chloroform (99%+) for spectroscopy were purchased from Acros Organics (Geel, Belgium)

Animals and Dosing—Male C57BL/6 mice were purchased from the Jackson Laboratory (Bar Harbor, ME) and male Wistar rats were purchased from Harlan (Indianapolis, IN, USA). In this study 12 male C57BL/6 mice and 6 male Wistar rats were separated into 3 groups (n=6 for each group). Each group of 6 animals was further divided into a treatment group (n=3) and a control group (n=3). The intragastric ethanol infusion of mice and rats was described previously[8⁻11].

Briefly, at the initial ethanol dose, total caloric intake derived from diet and ethanol for both mice and rats was initially set at 568 cal/kg/day, and the caloric percentages of ethanol, dietary carbohydrate (dextrose), protein (lactalbumin hydrolysate), and fat (corn oil) were 24.3%, 15.7%, 25%, and 35%, respectively. The daily ethanol dose was increased gradually

from week 1 to week 4. The highest caloric percentage of ethanol at the end of 4 weeks accounted for 34.4% of total calories. Adequate vitamin and salt mix were included at the amounts recommended by the Committee on Animal Nutrition of the National Research Council (AIN-76A, 4.42 g/L, and 15.4 g/L, respectively, Dyets Inc, PA). The animals were treated in accordance with the Guide for Care and Use of Laboratory Animals (NIH, Bethesda, MD, Publication 86-23, 1985).

Samples and Sample Processing—Liver samples were collected from control and alcohol-fed mice and rats and were frozen immediately on collection and stored on dry ice (solid carbon dioxide). The samples were then shipped on dry ice, being stored frozen at -80°C on receipt until extraction for analysis, at which point they were allowed warm sufficiently to enable an small amount (ca. 50 mg) to be removed and weighed. The sample for analysis was then immediately refrozen with dry ice until solvent extraction was performed, which was performed as soon as possible after aliquoting (within 20 min). For extraction the frozen samples were placed in Eppendorf tubes, homogenized and extracted with 1mL of H_2O/ACN, 50:50 (V/V), for 10 min in an ultrasonic bath (Ultrawave, Cardiff, UK).

The presence of ACN in the extraction medium serves to both aid in the solubilization and recovery of medium to non-polar metabolites and to precipitate proteins (thereby also inactivating hydrolytic enzymes). The samples were then centrifuged for 10 min at 20,800g (Centrifuge 5417C, Eppendorf AG, Hamburg, Germany). The pellets obtained *via* this process were re-suspended in 1.5 mL of $CHCl_3$/MeOH, 3:1 (V/V) and were then extracted for 10 min in the ultrasonic bath in order to obtain the nonpolar metabolite fraction for profiling. After centrifugation 1.3 mL of the clear supernatant was transferred to glass vials and left over night at room temperature in a fume cupboard to allow the solvents to evaporate. These samples were then re-dissolved in 1.3 mL of MeOH and also stored at -20°C until LC/MS analysis. Quality control (QC) samples for these organic extracts were prepared by pooling aliquots of 40 μL of each sample.

Liver Total Cholesterol—As reported in detail elsewhere [11], liver total cholesterol was determined using the Infinity Cholestero Reagent Kit (Sigma Diagnostics, St Louis, MO, USA).

Sample Analysis by LC-MS—Both rat and mouse-derived liver extracts were analyzed, in a randomized order by LC/MS using a quadrupole ion trap-time of flight mass spectrometer (LCMS-IT-TOF, Shimadzu Corporation) using data dependent acquisitions in electrospray ionization (ESI) in both positive and negative mode. To identify biologically significant components, high mass accuracy MS and MS^n fragment ion information was used to identify the most likely candidate formula.

Prior to analysis, ten pooled QC samples were run to "condition" and provide assurance that the system was suitable for use. During the analytical run itself one of these pooled QC samples was interspersed between every five biological samples.

For analysis 1.0 μL aliquots of each sample (maintained at 4°C in the autosampler) were injected for separation by HPLC, using gradient elution, with a Prominence LC system (Shimadzu Corporation, Kyoto, Japan) on an Acquity BEH C18 column (2.1 × 50mm; particle size 1.7 μm) at a flow rate of 0.4 mL min^{-1}, with the column maintained at 60°C. The chromatographic system used a binary solvent system delivered as a gradient of Solvent A (formic acid solution 0.1%) and Solvent B (methanol + 0.1% formic acid). The initial gradient conditions were 95% A: 5% B for 0.75 min followed by a step curvi-linear gradient up to 95% B over the next 15 min. The solvent composition was then held at 100% B for 6.5

min after which the column was returned to 5% B over the next 2.5 min, making a total cycle time of 25 min per sample.

Mass Spectrometry

All MS and MS^n mass spectra were acquired on a quadrupole ion trap-time of flight mass spectrometer (LCMS-IT-TOF, Shimadzu, Kyoto, Japan) equipped with an electrospray source. This instrument is based upon the ability of a quadrupole ion trap to deliver MS^n capability and the time of flight mass analyzer to support accurate mass measurements. The mass range is *m/z* 50-5000 in MS mode and *m/z* 50-3000 for MS^n experiments.

The following method parameters were used for sample analysis; mass range of *m/z* 150-1000 in MS and between *m/z* 50-1000 in MS^n mode; ion source temperature of 250°C; heated capillary temperature of 230°C; electrospray voltage of 4.5 kV; electrospray nebulisation gas flow was 1.5 L/minute; detector voltage 1.75 kV; ion accumulation time was 10 msec. Automated data dependent functions were set to acquire 5 scans for each precursor detected using the most intense ion signal as the trigger. Positive and negative ion mode were also used with a polarity switching time of 100 msecs.

Mass calibration was carried out using a trifluoroacetic acid sodium solution (2.5 mmol L^{-1}) from 50 to 1000 Da. Data acquisition and processing used software LCMS Solution 3.50.

Data Analysis

Profiling Solution software (Shimadzu Corporation, Kyoto, Japan) was used to create an aligned data array of retention time, *m/z* and intensity data for both positive and negative ion data. Profiling Solution has been developed using a unique algorithm to generate a spectral alignment data matrix followed by chromatographic integration and filtering. The algorithm performed dynamic binning of 'likely' high resolution accurate mass spectral ions for both positive and negative ion data streams which were combined and reduced into a retention time-aligned spectrum ion intensity matrix (ion intensity in this context refers to the peak height of the ion in the mass spectrum) before final reduction into a profiling chromatographic matrix of ion areas. Data processing takes into account spectral processing parameters (mass window and retention time tolerance, ion intensity threshold and a parameter to adjust the isomer valley threshold) and chromatogram processing parameters (including QC filtering which considers a minimum number of pooled ions required for an ion to be included in the matrix together with limits for ion signal intensity and retention time variability (%RSD), sample group related parameters which can be applied to limit the Pval threshold).

In this study, sample data was acquired using polarity switching mode. Profiling Solution software generated an aligned data array of both positive and negative ion MS data which was subsequently exported to SIMCA-P (Umetrics, MKS Instruments Inc., Sweden) for PCA analysis. Following noise reduction thresholding, a data array was processed using SIMCA-P and scaled to unit variance (the base weight is computed as 1/sdj, with sdj is the standard deviation of variable j computed around the mean). No variable was excluded in this analysis.

Metabolite features were statistically tested for their quantitative significance by considering the reproducibility of the ion signal in the pooled QC sample. In order to find the major ions contributing to group differences these data were analyzed by OPLS-DA. Two groups were defined (alcohol treated and control) and were put in two classes. The OPLS-DA S-plot combined the traditional loading plot and column plot confidence limits highlighting the ions of most significance. The x-axis provides a measure of the contribution of an ion whilst the y-axis provides a measure of correlation on an ion to the model. Ions furthest from the x-

axis and y-axis are both the highest contributors to differences between groups and also have the highest confidence in correlation to the model. Once a metabolite feature was identified the next stage was to confirm the metabolite identity using empirical formula prediction software and external data bases.

Formula Prediction Software

To verify component identification, the Formula Predictor software was used (Shimadzu Corporation, Kyoto, Japan). Predicting a candidate list based on MS and MS^n data takes into account a number of variables, including isotopic profile analysis, mass accuracy and mass resolution of the experimentally derived pseudo-molecular peak and related fragment ion data.

Metabolite Identification

Ions of significant interest were searched against external databases including; The Human Metabolome Database [www.hmdb.ca/], PubChem [http://pubchem.ncbi.nlm.nih.gov/], Biospider [http://biospider.ca/], LipidMaps [http://www.lipidmaps.com/], KEGG [http://www.genome.jp/kegg]. Database candidates were confirmed using Formula Prediction software (Shimadzu, Kyoto, Japan) to analyse isotopic profiles of MS data.

Positive and negative ion MS/MS data allowed a greater number of metabolites to be identified with a higher degree of confidence. In the case of fatty acyl metabolites the reference library in LipidMaps was acquired using only negative ion data whereas positive ion data was used to identify other metabolites by comparison with databases such as HMDB, MetLin and KEGG. Despite the limited MS/MS information in many databases and the differing instrument platforms (triple quadrupoles, Q-TOF, ion trap technologies) the MS/MS information was critical to a high confidence metabolite identification. In the case of phosphatidylethanol homologues and certain fatty acid ethyl esters metabolite identification was confirmed by reference to published literature.

Metabolite Confirmation

In order to confirm, or refute, the putative identities obtained *via* data base searches and mass spectrometric investigations a number of compounds were obtained as authentic standards for ions of significant interest. This enabled their chromatographic and mass spectrometric characteristics to be matched against the provisional identities derived from the sample-derived data.

Results

Pooled QC sample analysis was used to assess the performance of the system by repeatedly injecting the QC sample throughout the analytical run every 5 samples (see refs. 15-17). PCA analysis of the data set resulting from the profiling of the liver samples showed the QC samples to be tightly clustered together, with no obvious run order effects, for both positive and negative ESI data. An example of the PCA result is shown in Figure 1 for the combined positive and negative ion data array. The data from the QC samples were then interrogated to determine the number of ions present in the samples, their intensity and their % RSD values. The aligned data array for both positive and negative ion MS data was filtered using the pooled QC samples; ion signals with high variability in ion signal intensity and/or variance in peak retention time were not used in the data analysis. In line with the recommendations of the FDA for biomarker analysis18-19 ions showing % RSDs less than 30 were used in the subsequent analysis of the test and control animal sample data. Thus, the pooled QC filters were applied so that an ion should be present in at least 70% of the QC samples and have a variability of lower than 30% RSD (peak area) and 2% RSD (retention

time). Profiling Solution software produced a data array of 4963 ions that met the above criteria for a combined array for positive and negative ion data (1069 ions detected in negative ion; 3894 ions detected in positive ion; some 6239 ions were discarded as they did not meet the QC criteria). The QC data for the ions that met the required acceptance criteria are provided in supplementary Table S1 for positive and negative ESI results.

Control and Alcohol-treated Rat and Mouse Liver Metabolomes

As can be seen from the PCA analysis for the combined data array of positive and negative ion data shown in Figure 1, LC-MS of these extracts clearly enabled differentiation between the control groups for each species and between treatments. In the case of the mouse two separate investigations were performed with 3 mice/group. However, the data for both investigations showed consistent clustering between control and treated animals, indicating a similar metabolic response and thereby demonstrating the repeatability of the intragastric alcohol infusion dosing model in the mouse.

Major ions, highlighted by statistical methods such as OPLS-DA (Figure 2), that contributed to these phenotypic differences between the liver metabolomes of the two species corresponded to the distribution of fatty acyl metabolites (identification confirmed using the negative ion MS and MS/MS data corresponding to metabolites in the LipidMaps data base), fatty acid ethyl esters (identification of positive ion MS and MS/MS data in agreement with published data), glycerolipids (in agreement with positive ion mass accuracy data using KEGG, Human Metabolome Data Base and LipidMaps) and phosphatidylethanol (PEth) homologues (metabolites were identified by agreement with published MS/MS data using authentic standards) (Figure 3 and Figure 4).

With respect to the effects of ethanol treatment on the liver metabolomes unique marker ions for the intragastric alcohol-fed model were identified by positive ion detection at *m/z* 333.2788, 357.2788, 309.2788 and 311.2945 [M+H]$^+$ corresponding to fatty acid ethyl esters, ethyl arachidonate, ethyl DHA (docosahexaenoic acid), ethyl linoleate and ethyl oleate. Authentic standards were used to identify ethyl arachidonate and ethyl oleate.

Metabolites that were significantly down-regulated by alcohol treatment in both rat and mouse livers (particularly in mice) included the ion signal at *m/z* 369.3516 eluting with a retention time of 10.74 min (Figure 3). Using only the molecular ion as part of the automated search criteria against several data bases (KEGG, LipidMaps, Metlin) resulted in the mis-identification of this metabolite as the most likely identity was given as 3-deoxyvitamin D3 ([(5Z,7E)-9,10-seco-5,7,10(19)-cholestatriene, LMST03020618; MetLin MID 42544; PubChem: 49703700, molecular formula C27H44). However, comparison of this ion with the retention time of the authentic 3-deoxyvitamin D3 standard, which was observed to elute at 14.93 min., showed that it differed markedly from the ion signal in the liver samples. Further investigation demonstrated that the unknown metabolite matched both retention time and MS/MS spectra for cholesterol ((3β)-cholest-5-en-3-ol; *m/z* 369.3516 [M-H2O+H]$^+$). Thus, the mass spectrum for the authentic cholesterol standard was consistent with a positive ion base peak corresponding to a loss of water and MS/MS spectra dominated by the loss of a hydrocarbon structure.

Free cholesterol levels, as determined by a specific LC/MS based approach, were down-regulated in all alcohol treated mouse samples and in one rat sample. This is an interesting observation as the liver total cholesterol assessed with cholesterol esterase methods resulted in ~2 fold increase in the liver of alcohol infused mice and ~1.5 increase in the liver of alcohol infused rats11. In each of the samples with down-regulated free cholesterol amounts there was a corresponding increase in the amounts of cholesterol metabolites such as 7α-hydroxycholesterol (LipidMaps ID LMST01010013; cholest-5-en-3β,7α-diol; m/z 385.3465

[M+H -H2O]+) and 7-keto-cholesterol (LipidMaps ID; LMST01010049; 7-oxo-cholest-5-en-3β-ol; m/z 401.3414 [M+H]+. This overall increase in cholesterol-related material is in broad agreement with total cholesterol amounts measured using cholesterol esterase based methods. Clearly these effects on cholesterol metabolism would benefit from further, in depth, investigation of underlying molecular mechanisms.

Other metabolites that were down-regulated included retinol, a diacylglycerol isomer and cholesteryl eicosapentaenoic acid. (Figure 5)

Whilst the lipid profiles were broadly similar in both mouse and rat models there were a number of significant differences particularly in the up- and down-regulation of specific fatty acyl metabolites in the mouse. It was also interesting to note that retinol and cholesterol were both markedly down-regulated in the mouse following alcohol treatment compared to the rat. (Table 1).

Clinical biomarkers for alcohol exposure in man that have been considered include a number of minor conjugated ethanol metabolites such as ethyl glucuronide[20], ethyl sulphate [21], fatty acid ethyl esters[22] and homologues of phosphatidylethanol (PEth)[23]. PEth is an ethanol-derived phospholipid formed from phosphatidylcholine (PC) in cell membranes by a transphosphatidylation reaction catalyzed by phospholipase D. Previous studies have reported that the two predominant PEth species to monitor clinically would be 16:0/18:1 and 16:0/18:2, as these together accounted for approximately 60% of the total amount in blood from heavy drinkers. In the intragastric ethanol feeding model, the dominant PEth homologues detected in the alcohol treated liver samples were PEth 18:0/18:2 and PEth 16:0/18:2 for both rat and mouse (Table 1). PEth 18:0/18:2 and PEth 16:0/18:2 were identified by negative ion MS accurate mass and MS/MS spectrum. PEth 18:0/18:2 was confirmed by accurate mass *m/z* 727.5283 [M-H]⁻ and fragment ion data *m/z* 283.2643 (18:0) [C18H36O2] and 279.2330 (18:2) [C18H32O2]. Similarly, PEth 16:0/18:2 was identified by high mass accuracy MS data, *m/z* 699.4970 [M-H]⁻ and fragment ion data corresponding to *m/z* 255.2330 (16:0) [C16H32O2] and *m/z* 279.2330 (18:2) [C18H32O2]. In most control liver samples, PEth homologues were not detected.

Discussion

In an earlier study that used ¹H NMR spectroscopy to study ethanol-induced metabolic changes in liver, brain and serum from rats exposed to either a single dose or a chronic 4 day "binge" protocol of ethanol administration, decreased amounts of glucose, lactate, and alanine were measured in both liver and serum compared to control[12]. The decreases in the concentrations of some metabolites were combined with increased quantities of acetate in both liver and serum and an associated increase in acetoacetate only in serum. The 4-day chronic administration also increased β-hydroxybutyrate in liver whilst decreasing betaine concentrations. In a subsequent study urine and liver extracts from male C57BL/6J mice were analysed by ¹H NMR resonance spectroscopy and positive ion electrospray infusion/FTICR-MS to determine the biochemical changes resulting from chronic alcohol administration for up to 36 days[13]. In this study mice were fed an isocaloric control- or alcohol containing liquid diet (initially 7 g/kg/day rising to a final dose of 21 g/kg/day). Steatohepatitis was observed in the alcohol-fed group evidence by a 5-fold rise in serum alanine aminotransferase activity and a 6-fold increase in liver necrosis, inflammation and steatosis. Increased lipid peroxidation in the livers of the ethanol-dosed animals was also seen as well as (amongst others) increased acetate, alanine, lactate and carnitine by ¹H NMR spectroscopy and 7,10,13,16-docosatetraenoic acid, 3α,20β-preganediol and 11,14-eicosadienoic acid by FTICR-MS. In the organic extract the ESI-FTICR analysis detected some 300 metabolites reproducibly.

In the present study the use of LC-MS with both positive and negative ESI modes resulted in the repeatable detection of some 4963 ions some of which showed clear changes in response to alcohol administration. Here both positive and negative ESI were employed with success for the detection and identification of metabolites. Thus we found that fatty acyl identities could be clearly distinguished using the Lipid Maps data base using negative ion mode (in the case of the fatty acyl metabolites, LipidMaps has MS/MS spectra in negative ion mode only). Polarity switching during the run was a critical discriminator enabling high confidence identification in negative ion mode (anion attachment in negative ion ESI-MS is less likely than cation attachment in positive ion ESI-MS and enables automated software routines to identify metabolites using deprotonated molecular information) whilst providing information on other major ions in positive ion mode, such as cholesterol, which was significantly lower in mouse liver extracts, and somewhat reduced in the rat. The challenge, as was indeed the case for cholesterol, was in providing high confidence metabolite identification simply by reference to external data bases. In this study, mass accuracy alone did not provide a unique high confidence assignment especially where there are numbers of isobaric of isomers for particular atomic compositions. It is also important to note that positive ion MS/MS data for fatty acyl-metabolites are not yet included in the Lipid Maps data base. However, as is clear from the data presented in Table 1 there were numerous changes in non-polar metabolite profiles as a result of alcohol administration. Some of these changes appear to provide unique markers of alcohol administration in one species or another.

Thus, in the case of the rat the presence of metabolites corresponding to the fatty acid ethyl esters, ethyl arachidonate, ethyl DHA (docosahexaenoic acid), ethyl linoleate and ethyl oleate would provide a unique signature of alcohol exposure, being absent in the controls. These same metabolites, whilst (with the exception of ethyl DHA) present in small amounts in the extracts obtained from mouse livers were also greatly enhanced in concentration following alcohol administration showing more than 10 fold increases (see Table 1). Other up-regulated metabolites included eicosapentaenoic acid (5 and 6 fold change in mouse and rat respectively), gamma-linolenic acid (GLA) (3 fold change in the rat), monoarachidonic acid triglyceride (3 and 6 fold change in mouse and rat respectively) and a possible isomer of diacylglycerol (16 and 7 fold) (Table 1). Whilst in most cases the changes in relative metabolite concentrations were the same for both species there were differences in the response to alcohol administration. The most striking change was observed for retinol palmitate and retinol in alcohol treated mice. In these samples, retinol palmitate and retinol were not detected in any alcohol treated sample (both metabolites form m/z 269.2264 as a positive ion, the retention time and MS/MS spectra matched the authentic standard). Free cholesterol was also markedly lower in alcohol treated mouse (10 fold reduction in cholesterol levels compared to the control group; the identification was verified using the authentic standard). This change was also noted in the rat to a lesser extent. Fatty acyl metabolites such as docosapentaenoic acid (DPA, clupanodonic acid), arachidonic acid (AA) and adrenic acid were up-regulated in the rat but down-regulated in the mouse (Table 1).

In this study the change in metabolite profiles between animals and treatment groups has been measured as relative changes in ion signal intensity (peak area) to identify potential biomarkers. As part of further studies the development of fully quantitative assays for selected biomarkers will be required in order to better assess their value in understanding these models of alcohol-induced liver injury in rodents. Proposed clinical biomarkers for ethanol consumption in man include the conjugated minor ethanol metabolites ethyl glucuronide and ethyl sulphate, fatty acid ethyl esters and fatty acid ethyl esters and PEth. PEth is not a single molecular species but a group of phospholipids with a common nonpolar phosphoethanol head group onto which 2 fatty acid moieties, typically with a chain length of

16, 18, or 20 carbons are attached at positions sn-1 and sn-2. In the alcohol treated liver samples of both rat and mouse, PEth 18:0/18:2 and PEth 16:0/18:2 metabolites were detected and identified by high mass accuracy negative ion MS and MS/MS data. This result is in broad agreement with blood sample data taken from alcoholic patients[24].

Conclusions

In this study, mass spectrometry-based metabolite profiling was used to identify changes in endogenous metabolite levels in intragastric alcohol-fed mice and rats models using high accuracy MS^n analysis. Endogenous metabolites were measured and identified using a combination of high accuracy polarity switching MS/MS data, acquired on a LCMS-IT-TOF system, and verified by reference authentic standards and to internal and external databases ((http://www.lipidmaps.org; http://www.hmdb.ca; http://www.genome.jp/kegg/).

The study clearly showed a marked difference between the liver lipid profiles of alcohol treated mouse and rat samples with controls. The lipid profiles of mouse and rat liver samples undergo complex changes in lipid synthesis particularly with fatty acid ethyl esters, fatty acyls, glycerolipids and phosphatidylethanol homologues. Changes in liver lipid profiles in the intragastic ethanol model were consistent with clinical biomarkers used in monitoring alcohol-dependent patients during treatment.

Supplementary Material

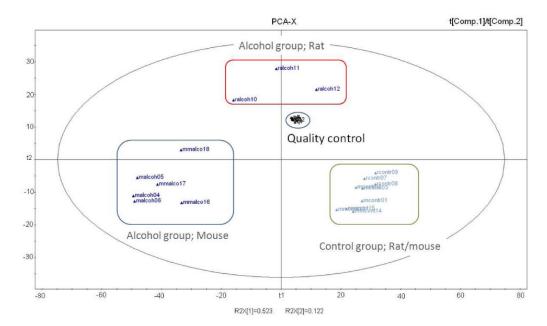Refer to Web version on PubMed Central for supplementary material.

Acknowledgments

References

1. Nicholson JK, Lindon JC, Holmes E. Xenobiotica. 1999; 29:1181–1189. [PubMed: 10598751]

2. Nicholson JK, Connelly J, Lindon JC, Holmes E. Nat Rev Drug Discov. 2002; 1:153–161. [PubMed: 12120097]

3. Fiehn O. Plant Molecular Biology. 2002; 48:155–171. [PubMed: 11860207]

4. Gavaghan CL, Holmes E, Lenz E, Wilson ID, Nicholson JK. FEBS Letters. 2000; 484:169–174. [PubMed: 11078872]

5. Lenz EM, Wilson ID. Journal of Proteome Research. 2007; 6:443–458. [PubMed: 17269702]

6. Theodoridis G, Gika HG, Wilson ID. TrAC - Trends in Analytical Chemistry. 2008; 27:251–260.

7. Wu Z, Huang Z, Lehman R, Zhao C, Xu G. Chromatographia. 2009; 69(suppl):S23–S32.

8. Tsukamoto H, Reidelberger RD, French SW, Largman C. Am J Physiol. 1984; 247:R595–R599. [PubMed: 6433728]

9. Tsukamoto H, Gaal K, French SW. Hepatology. 1990; 12:599–608. [PubMed: 2205558]

10. Tsukamoto H, Mkrtchyan H, Dynnyk A. Methods Mol Biol. 2008; 447:33–48. [PubMed: 18369909]

11. Shinohara M, Ji C, Kaplowitz N. Hepatology. 2010; 51:796–805. [PubMed: 20069651]

12. Nicholas PC, Kim D, Crews FT, Macdonald JM. Chem Res Tox. 2008; 21:408–420.

13. Bradford BU, O'Connell TM, Han J, Koysk O, Shymonyak S, Ross PK, Winnike J, Kono H, Rusyn I. Toxicol Appl Pharmacol. 2008; 232:236–243. [PubMed: 18674555]

14. Manna SK, Partterson AD, Yang Q, Krausz KW, Li H, Idle J, Fornace AJ Jr, Gonzalez FJ. J Proteome Res. 2010 in press.

15. Gika HG, Theodoridis GA, Wingate JE, Wilson ID. J Proteome Res. 2007; 6:3291–3303. [PubMed: 17625818]

16. Gika HG, Macpherson E, Theodoridis G, Wilson ID. J Chromatography B. 2008; 871:299–305.

17. Want EJ, Wilson ID, Gika H, Theodoridis G, Plumb RS, Shockcor J, Holmes E, Nicholson JK. Nature Protocols. 2010; 5:1005–1018.

18. FDA. Guidance for Industry, Bioanalytical method Validation. Food and Drug Administration, Centre for Drug Evaluation and Research (CDER); May. 2001 A guidance

19. Viswanathan CT, Bansal S, Booth B, DeStefano AJ, Rose MJ, Sailstad J, Shah VP, Skelly JP, Swann PG, Weiner R. Am Assoc Pharm Sci. 2007; 9:E30–E42.

20. Wurst F, Kempter C, Seidl S, Alt A. Alcohol and Alcoholism. 1999; 34:71–77. [PubMed: 10075405]

21. Wurst FM, Dresen S, Allen JP, Wiesbeck G, Graf M, Weinmann W. Addiction. 2006; 101:204–211. [PubMed: 16445549]

22. Laposata M. Addiction Biol. 1998; 3:5–14.

23. Gustavsson L. Alcohol Alcoholism. 1995; 30:391–406.

24. Helander A, Zheng Y. Clinical Chemistry. 2009; 55:1395–1405. [PubMed: 19423735]

Figure 1.
Multivariate statistics were performed on the aligned dataset of positive and negative ions using Umetrics SIMCA-P+ software. The treated groups and controls were clearly separated in this PCA data analysis.
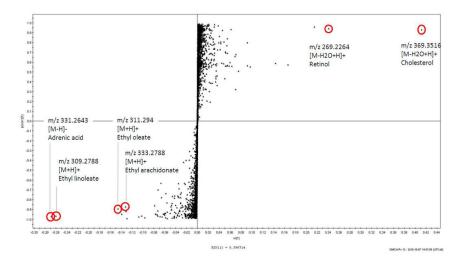
Figure 2.
The 's-plot' is generated in the SIMCA-P+ software to help generate a list of ions that significantly differed between the control group and alcohol treated group. Ions of interest were identified using molecular formula prediction tools, comparison with MS/MS spectra and by querying existing data bases. (The 's-plot' is presented for mouse liver samples, however, it is in broad agreement with rat liver metabolite profiles).
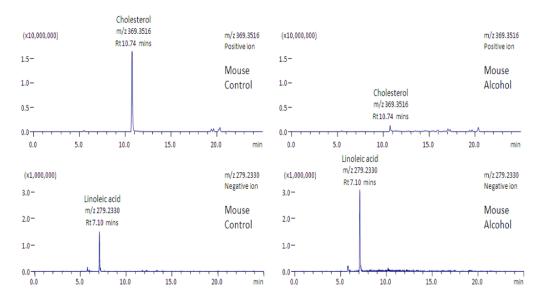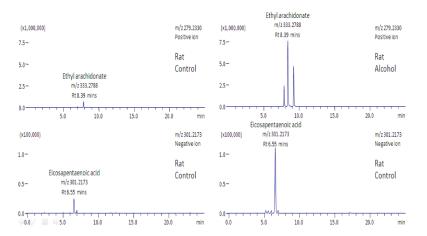
Figure 3.
Mass chromatograms for cholesterol (upper chromatogram; m/z 369.3516 (M-H2O+H$^+$) in positive ion mode) and linoleic acid (lower chromatogram; m/z 279.2330 (M-H)$^-$ in negative ion mode) in the mouse for both the control and treated group. Cholesterol was down regulated in the alcohol treated mouse together with retinol palmitate and retinol whilst fatty acids such as linoleic acid and fatty acid ethyl esters were markedly up regulated.

Figure 4.
Mass chromatograms for ethyl oleate (upper chromatogram; m/z 311.2945 (M+H)+ in positive ion mode) and eicosapentaenoic acid (lower chromatogram; m/z 301.2173 (M-H)⁻ in negative ion mode) in the rat for both the control and treated group. The metabolite profile in the rat was broadly similar to the mouse. Changes in rat liver fatty acyl metabolites such as eicosapentaenoic acid were in close agreement to the mouse. However, there were some interesting differences; ethyl oleate was not present in the rat control group but was detected in the mouse control group.
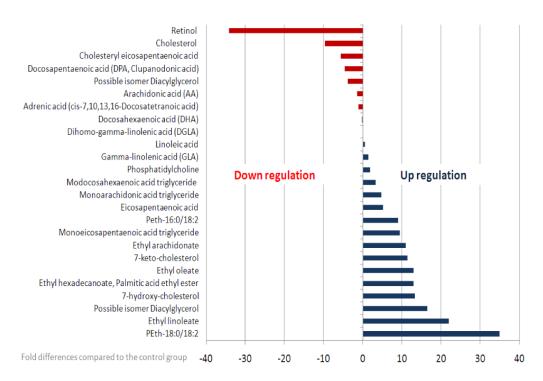
Figure 5.
The main metabolite classes to show major changes in the alcoholic liver-derived samples were fatty acyls, fatty acid ethyl esters, glycerolipids and phosphatidylethanol homologues. Significant metabolites that were up-regulated by alcohol treatment in both rat and mouse livers included fatty acyls metabolites such as octadecatrienoic acid and eicosapentaenoic acid, a number of fatty acid ethyl esters such as ethyl arachidonate, ethyl docosahexaenoic acid, ethyl linoleate and ethyl oleate and phosphatidylethanol (PEth) homologues (predominantly PEth 18:0/18:2 and PEth 16:0/18:2; PEth homologues are currently considered as potential biomarkers for harmful and prolonged alcohol consumption in man). (The figure presents data for the mouse only, however, metabolite profiles were broadly similar in both mouse and rat models).

Table 1

Significant changes in metabolite levels between the control group and alcohol treated mouse and rat. Metabolite identification was confirmed using authentic standards in the case of adrenic acid, cholesterol, ethyl arachidonate, ethyl oleate, retinol and retinol palmitate or by agreement with external MS and MS/MS data bases using both positive and negative ESI. The reproducibility of ion signal intensity was measured using a pooled QC sample injected throughout the run (n=6, interspersed between five biological samples). QC RSD variation was less than 10% for all metabolites measured in the samples). Ethyl DHA, ethyl octadecanoate, PEth-16:0/18:2 and PEth 18:0/18:2 were unique markers for liver samples treated with alcohol (these metabolites were not detected in the control group). The fold differences are measured as the difference between the average peak area for each treatment group compared to the control group for each animal. The average mass error for all reported metabolites was -0.71ppm (typical mass accuracy was less than 5ppm).

Accurate mass (m/z)	Rt (mins)	Ion	Formula	Identification	QC % RSD	Fold Differences		Data base reference	Supplementary information
						Mouse	Rat		
301.2173	6.55	[M-H]-	C20H30O2	Eicosapentaenoic acid	5.8	5	6	LMFA01030759	MS2; 203; 229; 257
277.2173	6.61	[M-H]-	C18H30O2	Gamma-linolenic acid	7.5	1	3	LMFA01030141	
269.2264	6.77	[M-H2O+H]+	C20H30O	Retinol	5.3	-34	-4	LMPR01090001	
327.2330	7.02	[M-H]-	C22H32O2	Docosahexaenoic acid	2.5	0	2	LMFA01030185	MS2; 229; 283; 299
303.2330	7.05	[M-H]-	C20H32O2	Arachidonic acid	1.5	-1	1	LMFA01030001	MS2; 205; 231; 259; 285
279.2330	7.10	[M-H]-	C18H32O2	Linoleic acid	4.7	1	2	LMFA01030120	
305.2486	7.46	[M-H]-	C20H34O2	Eicosatrienoic acid	5.6	0	6	LMFA01030158	MS2; 287
329.2486	7.53	[M-H]-	C22H34O2	Docosapentaenoic acid	3.0	-5	2	LMFA04000044	MS2; 231; 285; 311
331.2643	7.85	[M-H]-	C22H36O2	Adrenic acid	3.0	-1	6	LMFA01030178	MS2; 233; 281; 313
401.3414	8.26	[M+H]+	C27H44O2	7-keto-cholesterol	15.0	11	9	LMST01010049	MS2; 383; 365
357.2788	8.30	[M+H]+	C24H36O2	Ethyl DHA	6.2	Note 1	Note 1	CAS 1020718-25-5	
333.2788	8.39	[M+H]+	C22H36O2	Ethyl arachidonate	2.0	>11	Note 1	CAS 1808-26-0	Authentic standard
309.2788	8.48	[M+H]+	C20H36O2	Ethyl linoleate	1.1	>22	Note 1	CAS 544-35-4	
285.2788	8.95	[M+H]+	C18H36O2	Ethyl hexadecanoate,	9.9	>13	Note 1	CAS 628-97-7	
385.3465	9.00	[M-H20+H]+	C27H46O2	7-hydroxy-cholesterol	18.5	13	6	LMST01010013	
311.2945	9.21	[M+H]+	C20H38O2	Ethyl oleate	2.9	>13	Note 1	CAS 111-62-6	Authentic standard
313.3101	10.09	[M+H]+	C20H40O2	Ethyl octadecanoate	4.8	Note 1	Note 1	CAS 111-61-5	
369.3516	10.74	[M-H2O+H]+	C27H46O	Cholesterol	1.5	-10	-1	LMST03020618	Authentic standard
617.5140	12.96	[M+H]+	C39H68O5	Possible isomer Diacylglycerol	1.2	16	7	HMDB07675	Several possible isomers
786.6007	13.27	[M+H]+	C44H84NO8P	Phosphatidylcholine	5.7	2	1	HMDB08135	

Accurate mass (m/z)	Rt (mins)	Ion	Formula	Identification	QC % RSD	Fold Differences		Data base reference	Supplementary information
						Mouse	Rat		
667.5296	14.64	[M+H]+	$C_{43}H_{70}O_5$	Possible isomer Diacylglycerol	4.0	-4	-2	HMDB07769	Several possible isomers
269.2264	16.01	[M-C16H32O+H]+	$C_{36}H_{60}O$	Retinol palmitate	4.8	Note 2	-3	LMPR01090052	Authentic standard
699.4970	16.79	[M-H]-	$C_{39}H_{73}O_8P$	PEth-16:0/18:2	8.3	> 9	Note 1		Reference 24; MS2 ions
727.5283	19.02	[M-H]-	$C_{41}H_{77}O_8P$	PEth-18:0/18:2	8.1	> 35	Note 1		Reference 24; MS2 ions
901.7280	19.09	[M+H]+	$C_{59}H_{96}O_6$	Monoeicosapentaenoic acid triglyceride	1.6	9	20	HMDB10527	Several possible isomers
903.7436	19.60	[M+H]+	$C_{59}H_{98}O_6$	Monoarachidonic acid triglyceride	2.2	5	8	HMDB10523	Several possible isomers
671.5762	19.67	[M+H]+	$C_{47}H_{74}O_2$	Cholesteryl eicosapentaenoic acid	1.4	-6	-2	HMDB06731	Several possible isomers
905.7593	20.15	[M+H]+	$C_{59}H_{100}O_6$	Monoarachidonic acid triglyceride	2.1	3	6	HMDB10521	Several possible isomers

Note 1; no ion signal detected in the control group samples.

Note 2; no ion signal detected in the intra-gastric alcohol samples

LM; LipidMaps reference

HMDB; Human Metabolome Data Base